Published in final edited form as:
Genesis. 2014 September ; 52(9): 817–826. doi:10.1002/dvg.22795.

Generation of mice carrying a knockout-first and conditional-ready allele of transforming growth factor beta2 gene

A. S. Ishtiaq Ahmed[#], **Gracelyn C. Bose**, **Li Huang**, and **Mohamad Azhar**[*]
Program in Developmental Biology and Neonatal Medicine, Herman B. Wells Center for Pediatric Research, Indiana University School of Medicine, Indianapolis, IN 46202

Abstract

Transforming growth factor beta2 (TGFβ2) is a multifunctional protein which is expressed in several embryonic and adult organs. *TGFB2* mutations can cause Loeys Dietz syndrome, and its dysregulation is involved in cardiovascular, skeletal, ocular and neuromuscular diseases, osteoarthritis, tissue fibrosis, and various forms of cancer. TGFβ2 is involved in cell growth, apoptosis, cell migration, cell differentiation, cell-matrix remodeling, epithelial-mesenchymal transition, and wound healing in a highly context-dependent and tissue-specific manner. *Tgfb2*$^{-/-}$ mice die perinatally from congenital heart disease, precluding functional studies in adults. Here, we have generated mice harboring *Tgfb2*$^{\beta geo}$ (knockout-first *lacZ*-tagged insertion) gene-trap allele and *Tgfb2*^{flox} conditional allele. *Tgfb2*$^{\beta geo/\beta geo}$ or *Tgfb2*$^{\beta geo/-}$ mice died at perinatal stage from the same congenital heart defects as *Tgfb2*$^{-/-}$ mice. β-galactosidase staining successfully detected *Tgfb2* expression in the heterozygous *Tgfb2*$^{\beta geo}$ fetal tissue sections. *Tgfb2*^{flox} mice were produced by crossing the *Tgfb2*$^{+/\beta geo}$ mice with the FLPeR mice. *Tgfb2*$^{flox/-}$ mice were viable. *Tgfb2* conditional knockout (*Tgfb2*$^{cko/-}$) fetuses were generated by crossing of *Tgfb2*$^{flox/-}$ mice with *Tgfb2*$^{+/-}$;*EIIaCre* mice. Systemic *Tgfb2*$^{cko/-}$ embryos developed cardiac defects which resembled the *Tgfb2*$^{\beta geo/\beta geo}$, *Tgfb2*$^{\beta geo/-}$, and *Tgfb2*$^{-/-}$ fetuses. In conclusion, *Tgfb2*$^{\beta geo}$ and *Tgfb2*^{flox} mice are novel mouse strains which will be useful for investigating the tissue specific expression and function of TGFβ2 in embryonic development, adult organs, and disease pathogenesis and cancer.

Keywords

transforming growth factor *beta*; Loeys Dietz syndrome; cardiovascular; cancer; fibrosis; lung; blood; vascular; craniofacial; eye; wound healing; neurological; epithelial mesenchymal transition

Transforming growth factor beta2 (TGFβ2) belongs to a family of multifunctional proteins, known as the TGFβ superfamily (Akhurst and Hata 2012;Doetschman et al. 2012a;Arthur and Bamforth 2011). The other two mammalian isoforms of this superfamily are TGFβ1 and TGFβ3 (Azhar et al. 2009;Doetschman et al. 2012b). TGFβs play critical autocrine and/or paracrine roles in embryonic tissue development and maintenance of tissue homeostasis (Conway and Kaartinen 2011;Horiguchi et al. 2012). TGFβs are immunoregulatory and

[*]Correspondence to: Mohamad Azhar, 1044 W. Walnut St., Indianapolis, IN 46202; Telephone: 317-278-8661; mazhar@iu.edu.
[#]Current address: Department of Pharmacology and Toxicology, Medical College of Georgia, Georgia Regents University, Augusta

profibrotic cytokines that regulate cell growth, apoptosis, cell migration, cell differentiation, cell-matrix remodeling, epithelial-mesenchymal transition, and wound healing in a highly context-dependent and tissue-specific manner (Sonnylal et al. 2007;Soderberg et al. 2009;Kulkarni et al. 2002). Activated TGFβs interacts with TGFβ receptor type II and type I, which propagate the TGFβ signal into the cell by phosphorylating TGFβ receptor-specific canonical Smads (i.e., Smad2 and Smad3) and non-Smad mediators (e.g., TAK1, ERK MAPK) (Iwata et al. 2012;Yumoto et al. 2013;Akhurst and Hata 2012). The dysregulation of the TGFβ pathway leads to a number of human diseases and disorders, including tissue fibrosis and cancer (Akhurst and Hata 2012), underscoring the essential roles the TGFβ isoforms have *in vivo*.

TGFB2 mutations have been identified in Loeys-Dietz syndrome (LDS) (OMIM# 614816613795, 610380) (Lindsay et al. 2012;Boileau et al. 2012;Renard et al. 2012). Loeys-Dietz syndrome is a connective tissue disorder, predisposing individuals to serious cardiovascular, craniofacial, cutaneous, ocular, and skeletal complications (Loeys et al. 2013). The cardiovascular complications of LDS patients include congenital heart defects, aortic aneurysm, cardiomyopathy, and heart valve complications (Maccarrick et al. 2014). TGFB2 signaling is associated with cardiovascular complications of Kawasaki disease (Shimizu et al. 2011). TGFB2 levels are elevated in the myocardial tissue of the patients of dilated cardiomyopathy (Pauschinger et al. 1999). Furthermore, *TGFB2* is elevated in diseased mitral valves and aortas of Marfan syndrome patients, and mouse craniofacial defects, in which TGFβ signaling is also increased (Iwata, 2012 9286/id;Ng et al. 2004;Nataatmadja et al. 2006;Jain et al. 2009). Spatiotemporally restricted cardiac expression of *Tgfb2* and its overlap with *Tgfb1* or *Tgfb3* in various cardiac cell lineages including endocardial, myocardial, cardiac neural crest, and vascular smooth muscle cells in embryonic hearts (Dickson et al. 1993;Azhar et al. 2003;Molin et al. 2003) suggest a critical cell type specific autocrine-paracrine and synergistic roles of TGFβ2 in regulation of TGFβ signaling during cardiovascular development and remodeling. Systemic knockout mice of *Tgfb2* exhibit developmental defects in multiple organs and die at birth due to cardiac malformations, indicating that TGFβ2 is indispensable for embryonic tissue development (Sanford et al. 1997;Azhar et al. 2011;Bartram et al. 2001).

Here, we report on the generation and characterization of mice carrying a novel and flexible gene-trap knockout-first, *lacZ* tagged insertion allele of *Tgfb2* (hereafter referred to as $Tgfb2^{\beta geo}$). Three independent lines of the correctly targeted $Tgfb2^{\beta geo}$ ES cell clones were obtained from the European Conditional Mouse Mutagenesis Program (EUCOMM) for generating $Tgfb2^{\beta geo}$ mice. These ES clones had passed all rigorous quality control tests of the EUCOMM (Skarnes et al. 2011). $Tgfb2^{\beta geo}$ ES cell clones and $Tgfb2^{\beta geo}$ mice were validated by an extensive 5′ and 3′ screening (Fig. 1A–B). In this targeting scheme, homologous recombination can result in a $Tgfb2^{\beta geo}$ allele where gene function would be ablated by a polyadenylation (polyA) signal-mediated transcriptional stop at the end of the *lacZ* expression marker gene that is driven off the *Tgfb2* promoter. $Tgfb2^{+/\beta geo}$ mice were maintained on C57BL/6 genetic background. Genotyping analysis of the newborn offspring indicated that all $Tgfb2^{\beta geo/\beta geo}$ or $Tgfb2^{\beta geo/-}$ mice died at the perinatal stage (Fig. 1C, 2A–B). Timed-pregnant heterozygous $Tgfb2^{\beta geo}$ and $Tgfb2^{+/-}$ (C57BL/6) females that crossed

to heterozygous *Tgfb2*$^{\beta geo}$ males were used to produce embryos/fetuses for gross morphological and histological characterization. The data indicated that *Tgfb2*$^{\beta geo/\beta geo}$ and *Tgfb2*$^{\beta geo/-}$ fetuses at E16.5–E18.5 appeared grossly abnormal and exhibited abnormal body vasculature (Fig. 2A–B). Next, *Tgfb2* expression was measured in *Tgfb2*$^{\beta geo/\beta geo}$ hearts by real-time quantitative PCR (qPCR) via an intron spanning (exon 6–7) Universal ProbeLibrary assay. The data indicated that the amount of wild-type *Tgfb2* transcript containing the exon 6–7 was significantly downregulated in *Tgfb2*$^{\beta geo/\beta geo}$ fetal hearts compared to the wild-type fetuses (Fig. 2C). This suggests that although *Tgfb2* expression is abated, the polyA signal-mediated transcriptional stop at the end of the *lacZ* gene-trap cassette is not able to completely abolish the wild-type *Tgfb2* expression. Since we expected the *Tgfb2* promoter to drive the *lacZ* expression marker gene, the expression of *lacZ* was also analyzed by both RT-PCR, and β-galactosidase (X-gal) staining of fetal tissue cryo-sections. Limited data indicated remarkable *Tgfb2* expression associated with ossification within cartilage primordium of neural arch (Fig. 2E), mid-shaft region of left humerus (Fig. 2F), rib (Fig. 2G), and distal part of shaft of right ulna (Fig. H) during late embryonic development. The data confirmed the presence of *lacZ* expression as an indicator of the endogenous *Tgfb2* expression in *Tgfb2*$^{+/\beta geo}$ fetuses. Overall, as reported previously in *Tgfb2*$^{-/-}$ fetuses (Sanford et al. 1997), the significant loss of wild-type *Tgfb2* mRNA expression is consistent with the observed perinatal lethality of *Tgfb2*$^{\beta geo/\beta geo}$ or *Tgfb2*$^{\beta geo/-}$ mice.

Histological examination of serial tissue sections indicated multiple cardiac structural defects in *Tgfb2*$^{\beta geo/\beta geo}$ and *Tgfb2*$^{\beta geo/-}$ fetuses (Fig. 3A–H). *Tgfb2*$^{\beta geo/\beta geo}$ as well as *Tgfb2*$^{\beta geo/-}$ fetuses developed similar cardiac malformations of both the outflow tract and inflow tract. The outflow tract malformations of the mutant fetuses included double-outlet right ventricle (DORV) (100% cases), persistent truncus arteriosus (PTA) (27.2% cases), and abnormal morphology and thickening of aortic and/or pulmonary valves (100% cases) (Fig. 3A–D). In addition, the mutant fetuses developed double-inlet left ventricle (DILV) and/or overriding of tricuspid valves orifice via a perimembranous inlet ventricular septal defect (VSD) (100% cases), and abnormal morphology and thickening of tricuspid and mitral valves (100%) (Fig. 3E–H). Malformations of myocardium, epicardium, and aortic arch arteries also found but were not carefully determined in *Tgfb2*$^{\beta geo/\beta geo}$ or *Tgfb2*$^{\beta geo/-}$ fetuses. Notably, the overall penetrance of the observed cardiac valve and septal defects was significantly higher in *Tgfb2*$^{\beta geo/\beta geo}$ or *Tgfb2*$^{\beta geo/-}$ fetuses compared to *Tgfb2*$^{-/-}$ fetuses. We attribute this difference in the phenotypic penetrance between the *Tgfb2*$^{\beta geo/\beta geo}$ or *Tgfb2*$^{\beta geo/-}$ (C57BL/6) and *Tgfb2*$^{-/-}$ (129/BL-Swiss) (Azhar et al. 2011;Bartram et al. 2001) mice to different genetic background of the two strains. Collectively, our results show that *Tgfb2*$^{\beta geo/\beta geo}$ or *Tgfb2*$^{\beta geo/-}$ fetuses exhibit high penetrance of similar cardiac phenotypes that are reported previously in *Tgfb2*$^{-/-}$ fetuses. Thus, *Tgfb2*$^{\beta geo}$ allele represents a novel knockout-first, *lacZ*-tagged insertion and conditional-ready allele for *Tgfb2*.

Mice with conditional (*Tgfb2*^{flox}) allele were produced by crossing the conditional-ready *Tgfb2*$^{+/\beta geo}$ female mice with the Flp recombinase germline deleter (FLPeR) male mice (Farley et al. 2000), which removed the entire *FRT*-flanked *lacZ-neomycin* (βgeo) gene-trap cassette (Fig. 1A, C–E). Genomic PCR analysis confirmed that Flp recombinase resulted in

mice harboring *Tgfb2*^{flox} allele in which *loxP* sites flanked the exon 2 of *Tgfb2* (Fig. 1D–E). Subsequently, *Tgfb2*$^{flox/-}$ mice were produced by intercrossing the *Tgfb2*$^{+/flox}$ and *Tgfb2*$^{+/-}$ (C57BL/6) mice. *Tgfb2*$^{flox/-}$ and *Tgfb2*$^{flox/flox}$ mice were viable and fertile, and the adult *Tgfb2*$^{flox/-}$ mice were normal and indistinguishable from the wild-type littermate mice (Fig. 1D). In a proof of principle experiment, embryos with a *Tgfb2* conditional knockout (*Tgfb2*$^{cko/-}$) allele were generated by crossing the *Tgfb2*$^{flox/-}$ mice with *Tgfb2*$^{+/-}$;*EIIaCre* transgenic mice. *EIIaCre* mice have ubiquitous Cre activity and are known to generate germline or systemic knockout animals from the floxed animals (Holzenberger et al. 2000;Doetschman et al. 2012b). The data indicated that *EIIaCre* recombinase successfully excised the exon 2 of *Tgfb2 in vivo* (Fig. 4A). Histological and immunohistochemical analyses were done and the changes in cardiac structure and morphology were cataloged from the wild-type control, *Tgfb2*$^{flox/-}$;*EIIaCre*$^{-}$, and *Tgfb2*$^{flox/-}$;*EIIaCre*$^{+}$ (i.e., *Tgfb2*$^{cko/-}$) fetuses at E16.5–E18.5. Cross comparison of cardiac phenotype indicated that *Tgfb2*$^{cko/-}$ fetuses developed a spectrum of heart defects which resembled the *Tgfb2*$^{\beta geo/\beta geo}$, *Tgfb2*$^{\beta geo/-}$, and *Tgfb2*$^{-/-}$ fetuses (Fig. 4B–G). These data indicate that *Tgfb2*^{flox} mice are fully capable of producing robust conditional Cre-mediated deletion of *Tgfb2 in vivo*.

Systemic *Tgfb2* deletion studies by very nature are limited in scope, and leave a fundamental gap in our understanding of the critical cell-source of TGFβ2 (endocardium, neural crest and/or myocardium, second heart field, epicardium) as well as its regulatory mechanisms (canonical and/or non-canonical) that mediate cardiovascular development and remodeling. TGFβ2 is involved in adult cardiovascular pathologies including aortic aneurysm, cardiac fibrosis and cardiomyopathy, mitral valve prolapse, and calcific aortic valve disease. In addition, TGFβ2 plays important role in muscular, craniofacial, ocular, chronic liver, kidney, neurodegenerative and autoimmune diseases, osteoarthritis, tissue fibrosis, and various forms of cancer. The expression of *Tgfb2* in adult wild-type mouse cardiovascular tissues has not been determined yet. It is known that *Tgfb2* expression increases in diseased tissues, and many other pathophysiological states and cancer (Iwata et al. 2012;Lindsay et al. 2012;Friess et al. 1993). Collectively, *Tgfb2*$^{+/\beta geo}$ mice with *lacZ*-tagged insertion allele will be useful for localizing endogenous *Tgfb2* expression in embryos and adults, changes in *Tgfb2* expression and distribution in a longitudinal study in the pathogenesis of cardiovascular and other diseases, and in response to stress (i.e., Ang II, aortic coarctation, high fat diet) to induce cardiovascular disease states (e.g., aortic aneurysm, cardiac hypertrophy, atherosclerosis). Finally, *Tgfb2*^{flox} mice open a new frontier, and have unlimited potential to advance the understanding of TGFβ2 function in embryonic development, tissue homeostasis in adults, pathogenesis of cardiovascular and other diseases, and various forms of cancer. In conclusion, the generation and characterization of *Tgfb2*$^{\beta geo}$ and *Tgfb2*^{flox} mice is a major first step towards defining the tissue-specific expression and function of *Tgfb2* and TGFβ2 regulatory mechanisms in organ development, function, and disease.

Methods

Generation of *Tgfb2*$^{\beta geo}$ and *Tgfb2*^{flox} mice

All animal breeding and procedures are approved by the Institutional Animal Care and Use Committee (Indiana University School of Medicine). *Tgfb2*$^{\beta geo}$ mice will be made available to other investigators consistent with the general guidelines, policies, and procedures of the Indiana University. Mouse ES cells with *Tgfb2* knockout-first *lacZ* tagged insertion allele (ID:47128, Targeting Confirmed) are available to all non-profit non-commercial investigators through EUCOMM. Three independently targeted clones of *Tgfb2*$^{\beta geo}$ ES cells were obtained from the EUCOMM. The ES cells were male and heterozygous for the *Tgfb2*$^{\beta geo}$ allele. The specific details and the complete DNA sequence of the *Tgfb2*$^{\beta geo}$ gene targeting construct (L1L2_Bact_P) are available in the GeneBank (Accession# JN955293). *Tgfb2* is located on mouse chromosome 1 and has 7 exons (NCBI Gene ID# 21808). *Tgfb2*$^{\beta geo}$ is a targeted trap allele which functions as a gene-trap knockout (Skarnes et al. 2011). The targeting vector contained an IRES-*LacZ* trapping cassette and a floxed promoter-*neomycin* cassette inserted into an intron 1 of the *Tgfb2*. The mutagenic cassette had an Engrailed (En2) splice acceptor sequence and poly-A transcription termination signals which was expected to disrupt the *Tgfb2* function while expressing the *lacZ* gene under the control of the endogenous *Tgfb2* promoter for studying its gene expression. Mycoplasma testing and chromosome counting was done by EUCOMM. All *Tgfb2*$^{\beta geo}$ ES cell clones were mycoplasma negative. Also, chromosome counting had found no chromosomal abnormalities in *Tgfb2*$^{\beta geo}$ ES cell clones.

We validated the *Tgfb2*$^{\beta geo}$ ES cell clones by 3′ screen and 5′ screen for correct gene targeting using long range PCR (LR-PCR) method. These LR-PCR reactions amplified very large and specific PCR products, ranging from 3.9 kb to 7.4 kb in the *Tgfb2*$^{\beta geo}$ targeted clones. The 5′ LR-PCR had confirmed correct integration of the *Tgfb2* on the 5′ side by *Tgfb2*-specific 5′-outside *forward* primer (F74 or F75) and constant cassette specific 3′-reverse primer (R66 or R75). The subsequent 5′ LR-PCR product was sequenced with a primer to the upstream *FRT* to verify the *Tgfb2* and *FRT* site. In addition, the 3′ LR-PCR had confirmed the correct integration of the *Tgfb2* on the 3′ side by *Tgfb2*-specific 3′-outside *reverse* primer (R76 or R77) and constant cassette specific 5′-forward primer (F103, F76). The subsequent LR-PCR product was sequenced with a primer to the downstream *loxP* (*Tgfb2*-rev primer, R64) to verify the *Tgfb2* and *loxP* site. Two or more sets of LR-PCR assays were used in both 5′ and 3′ screen with similar results. The following primers were used in the LR-PCR 5′ screen: CTCCTGATCTCCAGTGATCTTGTGTAAC (F74, forward 5′-outside primer), GTGATATGTGCAATGTCTGATGTACTC (F75, forward 5′-outside primer), CACAACGGGTTCTTCTGTTAGTCC (R66, reverse universal/cassette primer). The following primers were used in the LR-PCR 3′ screen: GCAATAGCATCACAAATTTCACAAATAAAGCA (F103, forward universal/cassette primer), GAGATGGCGCAACGCAATTAATG (F76, forward universal/cassette primer), CAACACACATGGTTCCAACACCACCGCCG (R76, reverse 3′-outside primer), CTCACTATCCTTAGAGAGCTAAGCAAGC (R77, reverse 3′-outside primer). The following PCR conditions were used: denaturation: 93°C/3 min; annealing and amplification: 92°C/15 sec, 65°C/30 sec, 65°C/8 min (−1°C/cycle) for 8x; 92°C/15 sec,

55°C/30 sec, 65°C/8 min (+20 sec/cycle) for 30x; 65°C/9 min, 4°C hold. Phusion® High-Fidelity PCR Master Mix with HF Buffer (New England Biolabs, Inc) was used for amplifying the large PCR products in the both LR-PCR screens.

Strain of origin of *Tgfb2*$^{\beta geo}$ ES cell clones was C57BL/6N (Parental ES cell line: JM8) and the ES cells carried the genotype A/a (Agouti heterozygous). The dominant agouti coat color gene is restored in JM8 cells by targeted repair of the C57BL/6 nonagouti mutation (Pettitt et al. 2009). *Tgfb2*$^{\beta geo}$ ES clones were thawed and expanded, and the blastocysts (C57BL/6) injection and embryo transfer were done by Transgenic & Knockout-Mouse Core Facility (Indiana University School of Medicine). Based on percent coat color (agouti/black), several male chimeras were identified from blastocyst injections of both ES cell clones. At 7 weeks of age the *Tgfb2*$^{\beta geo}$ male chimeras were mated with C57BL/6 wild-type female mice, and a germ line transmission of *Tgfb2*$^{\beta geo}$ allele was successfully established. For genotyping of *Tgfb2*$^{\beta geo}$ mice, we used a *Tgfb2* specific primer in the 5′ homology arm (F65) with the constant/cassette primer (R66) in the targeting cassette to detect the *Tgfb2*$^{\beta geo}$ allele. Another *Tgfb2* specific primer was designed in the 3′ homology arm (R65) in order to detect the wild-type allele with a PCR fragment between the two *Tgfb2* specific primers. DNA sequence of some of the *Tgfb2* specific primers that were used for the genotyping includes: CACCTTTTACCTACAGATGAAGTTGC (F65, forward primer), CTTAAGACCACACTGTGAGATAATCC (R65, reverse primer). The following PCR conditions were used: denaturation: 95°C/3 min; annealing and amplification 95°C/30 sec, 60°C/30 sec, 72°C/30 sec for 35x, 72°C/3 min; 4°C hold.

For generation of mice with a *Tgfb2*^{flox} allele, *Tgfb2*$^{+/\beta geo}$ female mice were crossed to FLPeR mice. PCR primers and PCR conditions for genotyping FLPeR transgenic mice were used as recommended (Farley et al. 2000). For initial screening of *Tgfb2*^{flox} and *Tgfb2*$^{\beta geo}$ allele, *Tgfb2*-5′ arm (F65), constant cassette (R66), *Tgfb2*-3′arm (R65) PCR primers were used. In addition, two specific sets of PCR primers which identified *Tgfb2*^{flox} but not the *Tgfb2*$^{\beta geo}$ allele were used for further confirmation. These two independent PCR genotyping reactions used gene-specific (F86) and constant cassette (R86), and gene-specific forward (F86) and reverse (R88) primers, respectively. *Tgfb2*^{flox} female mice were crossed with *EIIaCre* deleter mice (Holzenberger et al. 2000). PCR genotyping for the *EIIaCre* transgenic pups were done as published (Doetschman et al. 2012b). Genomic PCR on tail DNA samples (F86 and R88) were used for detecting the Cre-mediated recombination in the *Tgfb2*$^{flox/-}$;*EIIaCre* mice. PCR genotyping for detecting *Tgfb2*$^{+/-}$ allele was performed as described (Sanford et al. 1997). DNA sequence of the additional primers that were used for the *Tgfb2*^{flox} or *Tgfb2*^{cko} allele genotyping included: AAGGCGCATAACGATACCAC (F86, forward primer), CCGCCTACTGCGACTATAGAGA (R86, reverse primer), ACTGATGGCGAGCTCAGACC (R88, reverse primer). The following PCR conditions were used for genotyping *Tgfb2*^{flox} or *Tgfb2*^{cko} allele: denaturation: 94°C/3 min; annealing and amplification 94°C/30 sec, 58°C/30 sec, 72°C/45 sec for 35x, 72°C/5 min; 4°C hold.

Histological, immunohistochemical and X-gal staining

Wild-type control and various groups of experimental embryos collected between E13.5 and E18.5 were processed for histological and molecular analyses as described (Azhar et al.

2011). Embryos were genotyped using genomic DNA extracted from tail biopsies. Hematoxylin and eosin staining was performed on 7-μm-thick serial sections of heart for routine histological examination (n=11 for E13.5–E18.5). Cardiac structure and morphology was determined by immunohistochemistry using cardiac myosin heavy chain (MF20) antibody (Developmental Studies Hybridoma Bank, Iowa). Tissue collection, processing, and β-galactosidase staining on 14 μm thick frozen (O.C.T.) tissue sections were done according to the published protocol (Komatsu et al. 2014). X-gal-stained tissue sections were counterstained with nuclear fast red (Vector Lab, Burlingame, CA). Images of whole embryos were captured in a stereozoom microscope (Zeiss Stemi 2000-C). All sections were visualized under brightfield optics with a Zeiss AxioLab.A1 light microscope (Carl Zeiss Microimaging, Inc.), and the morphometric measurements on the captured images were done by AxioVision Zeiss imaging software and NIH Image J (Fiji).

Real-time quantitative PCR Analysis

Real-time qPCR analysis (via intron spanning assay) was done using Universal ProbeLibrary (UPL) assay according to the manufacturer's protocols (Roche Inc, Indianapolis, IN). Expression of *lacZ* was detected using RT-PCR. Whole hearts from wild-type or *Tgfb2* gene-trap knockout or conditional knockout fetuses at E16.5 were collected under a stereozoom microscope (Zeiss Stemi 2000-C). Total RNA was isolated by RNeasy Mini kit (Qiagen, Valencia, CA). Three different samples of wild-type and experimental fetal hearts were assessed by real-time qPCR in LightCycler 480 (Roche Inc, Indianapolis, IN). ProbeFinder Assay Design Software (Roche Inc, Indianapolis, IN) was used to select the target-specific primer sequences and the matching Mouse Universal ProbeLibrary probe. Each reaction was performed in triplicate. The relative amount of target mRNA normalized to *β-actin* and to the wild-type was calculated. Specific primers and probes that were used in the qPCR or RT-PCR assays included: ATCACGACGCGCTGTATC (*lacZ* forward primer), ACATCGGGCAAATAATATCG (*lacZ* reverse primer), TGGAGTTCAGACACTCAACACA (*Tgfb2* exon 6-specific forward primer), AAGCTTCGGGATTTATGGTGT (*Tgfb2* exon 7-specific reverse primer), TCCTCAGC (*Tgfb2* exon 7-specific UPL probe #73). The UPL Reference Gene Assay for *β-actin* (#05046190001, Roche, Inc) was used for quantification of gene expression using dual-color real-time qPCR. The following conditions were used for *lacZ* PCR: denaturation- 94°C/5 min; annealing and amplification- 94°C/30 sec, 58°C/30 sec, 72°C/45 sec for 35x, 72°C/5 min; 12°C hold. For UPL qPCR, the following conditions were used: Pre-incubation: 95°C/4 min; Amplification: 95°C/10 sec, 60°C/30 sec, 72°C/01 sec for 45x; Cooling: 40°C/30 sec.

Statistical Analysis

All experiments were done on three or more embryos per genotype per developmental stage with similar results. Microsoft Excel was used for managing the raw data. Statistics was performed using pair-wise comparisons between the groups, utilizing analysis of variance and unpaired two-tailed t-test (SigmaPlot, Systat Software, Inc., CA). Data was reported as means ± SE of the mean. Probability values <0.05 were considered as significant.

Acknowledgments

Supported, in part, by the Indiana University Department of Pediatrics (Neonatal-Perinatal Medicine), Riley Children's Foundation, and Simmons Clinical Fund, Biomedical Research Grant (IU School of Medicine), and the Indiana CTSI pilot fund (via Grant # TR000006 from the National Institutes of Health, National Center for Advancing Translational Sciences, Clinical and Translational Sciences Award) grants (M.A.).

We thank the Transgenic & Knockout-Mouse Core Facility at the Indiana University School of Medicine and Mr. Bill Carter for generating the chimeric *Tgfb2*$^{\beta geo}$ mice.

LITERATURE CITED

Akhurst RJ, Hata A. Targeting the TGFbeta signalling pathway in disease. Nat Rev Drug Discov. 2012; 11:790–811. [PubMed: 23000686]

Arthur HM, Bamforth SD. TGFbeta signaling and congenital heart disease: Insights from mouse studies. Birth Defects Res A Clin Mol Teratol. 2011; 91:423–434. [PubMed: 21538815]

Azhar M, Brown K, Gard C, Chen H, Rajan S, Elliott DA, Stevens MV, Camenisch TD, Conway SJ, Doetschman T. Transforming growth factor Beta2 is required for valve remodeling during heart development. Dev Dyn. 2011; 240:2127–2141. [PubMed: 21780244]

Azhar M, Schultz JE, Grupp I, Dorn GW, Meneton P, Molin DG, Gittenberger-de Groot AC, Doetschman T. Transforming growth factor beta in cardiovascular development and function. Cytokine Growth Factor Rev. 2003; 14:391–407. [PubMed: 12948523]

Azhar M, Yin M, Bommireddy R, Duffy JJ, Yang J, Pawlowski SA, Boivin GP, Engle SJ, Sanford LP, Grisham C, Singh RR, Babcock GF, Doetschman T. Generation of mice with a conditional allele for transforming growth factor beta 1 gene. Genesis. 2009; 47:423–431. [PubMed: 19415629]

Bartram U, Molin DG, Wisse LJ, Mohamad A, Sanford LP, Doetschman T, Speer CP, Poelmann RE, Gittenberger-de GA. Double-outlet right ventricle and overriding tricuspid valve reflect disturbances of looping, myocardialization, endocardial cushion differentiation, and apoptosis in *Tgfb2* knockout mice. Circulation. 2001; 103:2745–2752. [PubMed: 11390347]

Boileau C, Guo DC, Hanna N, Regalado ES, Detaint D, Gong L, Varret M, Prakash SK, Li AH, d'Indy H, Braverman AC, Grandchamp B, Kwartler CS, Gouya L, Santos-Cortez RL, Abifadel M, Leal SM, Muti C, Shendure J, Gross MS, Rieder MJ, Vahanian A, Nickerson DA, Michel JB, Jondeau G, Milewicz DM. TGFB2 mutations cause familial thoracic aortic aneurysms and dissections associated with mild systemic features of Marfan syndrome. Nat Genet. 2012; 44:916–921. [PubMed: 22772371]

Conway SJ, Kaartinen V. TGFbeta superfamily signaling in the neural crest lineage. Cell Adh Migr. 2011; 5:232–236. [PubMed: 21436616]

Dickson MC, Slager HG, Duffie E, Mummery CL, Akhurst RJ. RNA and protein localisations of TGF beta 2 in the early mouse embryo suggest an involvement in cardiac development. Development. 1993; 117:625–639. [PubMed: 7687212]

Doetschman T, Barnett JV, Runyan RB, Camenisch TD, Heimark RL, Granzier HL, Conway SJ, Azhar M. Transforming growth factor beta signaling in adult cardiovascular diseases and repair. Cell Tissue Res. 2012a; 347:203–223. [PubMed: 21953136]

Doetschman T, Georgieva T, Li H, Reed TD, Grisham C, Friel J, Estabrook MA, Gard C, Sanford LP, Azhar M. Generation of mice with a conditional allele for the transforming growth factor beta3 gene. Genesis. 2012b; 50:59–66. [PubMed: 22223248]

Farley FW, Soriano P, Steffen LS, Dymecki SM. Widespread recombinase expression using FLPeR (flipper) mice. Genesis. 2000; 28:106–110. [PubMed: 11105051]

Friess H, Yamanaka Y, Buchler M, Ebert M, Beger HG, Gold LI, Korc M. Enhanced expression of transforming growth factor beta isoforms in pancreatic cancer correlates with decreased survival. Gastroenterology. 1993; 105:1846–1856. [PubMed: 8253361]

Holzenberger M, Lenzner C, Leneuve P, Zaoui R, Hamard G, Vaulont S, Bouc YL. Cre-mediated germline mosaicism: a method allowing rapid generation of several alleles of a target gene. Nucleic Acids Res. 2000; 28:E92. [PubMed: 11058142]

Horiguchi M, Ota M, Rifkin DB. Matrix control of transforming growth factor-beta function. J Biochem. 2012; 152:321–329. [PubMed: 22923731]

Iwata J, Hacia JG, Suzuki A, Sanchez-Lara PA, Urata M, Chai Y. Modulation of noncanonical TGF-beta signaling prevents cleft palate in Tgfbr2 mutant mice. J Clin Invest. 2012; 122:873–885. [PubMed: 22326956]

Komatsu Y, Kishigami S, Mishina Y. In situ hybridization methods for mouse whole mounts and tissue sections with and without additional beta-galactosidase staining. Methods Mol Biol. 2014; 1092:1–15.10.1007/978-1-60327-292-6_1.:1-15 [PubMed: 24318810]

Kulkarni AB, Thyagarajan T, Letterio JJ. Function of cytokines within the TGF-beta superfamily as determined from transgenic and gene knockout studies in mice. Curr Mol Med. 2002; 2:303–327. [PubMed: 12041733]

Lindsay ME, Schepers D, Bolar NA, Doyle JJ, Gallo E, Fert-Bober J, Kempers MJ, Fishman EK, Chen Y, Myers L, Bjeda D, Oswald G, Elias AF, Levy HP, Anderlid BM, Yang MH, Bongers EM, Timmermans J, Braverman AC, Canham N, Mortier GR, Brunner HG, Byers PH, Van EJ, van LL, Dietz HC, Loeys BL. Loss-of-function mutations in TGFB2 cause a syndromic presentation of thoracic aortic aneurysm. Nat Genet. 2012; 44:922–927. [PubMed: 22772368]

Loeys BL, Mortier G, Dietz HC. Bone lessons from Marfan syndrome and related disorders: fibrillin, TGF-B and BMP at the balance of too long and too short. Pediatr Endocrinol Rev. 2013; 10(Suppl 2):417–23. 417–423. [PubMed: 23858625]

Maccarrick G, Black JH III, Bowdin S, El-Hamamsy I, Frischmeyer-Guerrerio PA, Guerrerio AL, Sponseller PD, Loeys B, Dietz HC III. Loeys-Dietz syndrome: a primer for diagnosis and management. Genet Med10. 2014

Molin DG, Bartram U, Van der HK, Van Iperen L, Speer CP, Hierck BP, Poelmann RE, Gittenberger-de-Groot AC. Expression patterns of Tgfbeta1-3 associate with myocardialisation of the outflow tract and the development of the epicardium and the fibrous heart skeleton. Dev Dyn. 2003; 227:431–444. [PubMed: 12815630]

Pettitt SJ, Liang Q, Rairdan XY, Moran JL, Prosser HM, Beier DR, Lloyd KC, Bradley A, Skarnes WC. Agouti C57BL/6N embryonic stem cells for mouse genetic resources. Nat Methods. 2009; 6:493–495. [PubMed: 19525957]

Renard M, Callewaert B, Malfait F, Campens L, Sharif S, Del CM, Valenzuela I, McWilliam C, Coucke P, De PA, De BJ. Thoracic aortic-aneurysm and dissection in association with significant mitral valve disease caused by mutations in TGFB2. Int J Cardiol. 2012; 10

Sanford LP, Ormsby I, Gittenberger-de GA, Sariola H, Friedman R, Boivin GP, Cardell EL, Doetschman T. TGFbeta2 knockout mice have multiple developmental defects that are non-overlapping with other TGFbeta knockout phenotypes. Development. 1997; 124:2659–2670. [PubMed: 9217007]

Shimizu C, Jain S, Davila S, Hibberd ML, Lin KO, Molkara D, Frazer JR, Sun S, Baker AL, Newburger JW, Rowley AH, Shulman ST, Davila S, Burgner D, Breunis WB, Kuijpers TW, Wright VJ, Levin M, Eleftherohorinou H, Coin L, Popper SJ, Relman DA, Fury W, Lin C, Mellis S, Tremoulet AH, Burns JC. Transforming Growth Factor-{beta} Signaling Pathway in Patients With Kawasaki Disease. Circ Cardiovasc Genet. 2011; 4:16–25. [PubMed: 21127203]

Skarnes WC, Rosen B, West AP, Koutsourakis M, Bushell W, Iyer V, Mujica AO, Thomas M, Harrow J, Cox T, Jackson D, Severin J, Biggs P, Fu J, Nefedov M, de Jong PJ, Stewart AF, Bradley A. A conditional knockout resource for the genome-wide study of mouse gene function. Nature. 2011; 474:337–342. [PubMed: 21677750]

Soderberg SS, Karlsson G, Karlsson S. Complex and context dependent regulation of hematopoiesis by TGF-beta superfamily signaling. Ann N Y Acad Sci. 2009; 1176:55–69.10.1111/j.1749-6632.2009.04569.x.:55-69 [PubMed: 19796233]

Sonnylal S, Denton CP, Zheng B, Keene DR, He R, Adams HP, Vanpelt CS, Geng YJ, Deng JM, Behringer RR, de CB. Postnatal induction of transforming growth factor beta signaling in fibroblasts of mice recapitulates clinical, histologic, and biochemical features of scleroderma. Arthritis Rheum. 2007; 56:334–344. [PubMed: 17195237]

Yumoto K, Thomas PS, Lane J, Matsuzaki K, Inagaki M, Ninomiya-Tsuji J, Scott GJ, Ray MK, Ishii M, Maxson R, Mishina Y, Kaartinen V. TGF-beta-activated kinase 1 (Tak1) mediates agonist-

induced Smad activation and linker region phosphorylation in embryonic craniofacial neural crest-derived cells. J Biol Chem. 2013; 288:13467–13480. [PubMed: 23546880]

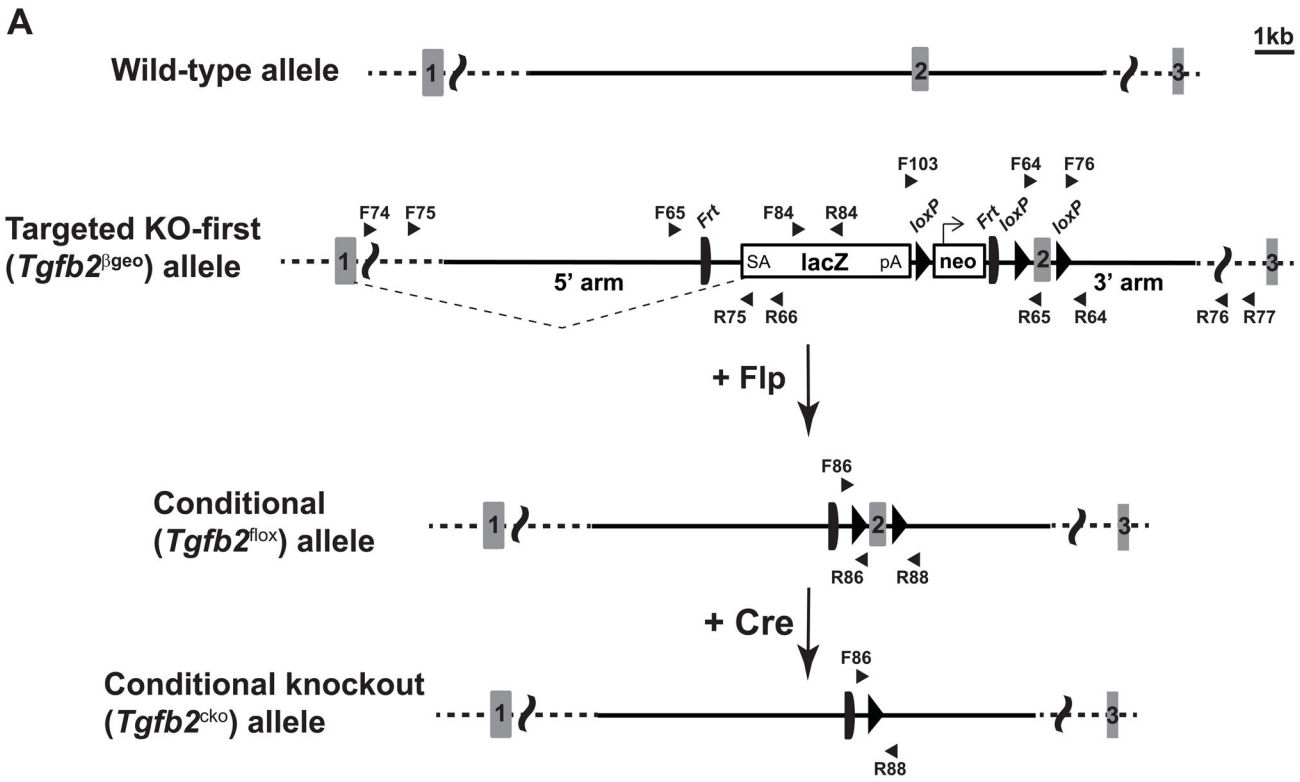

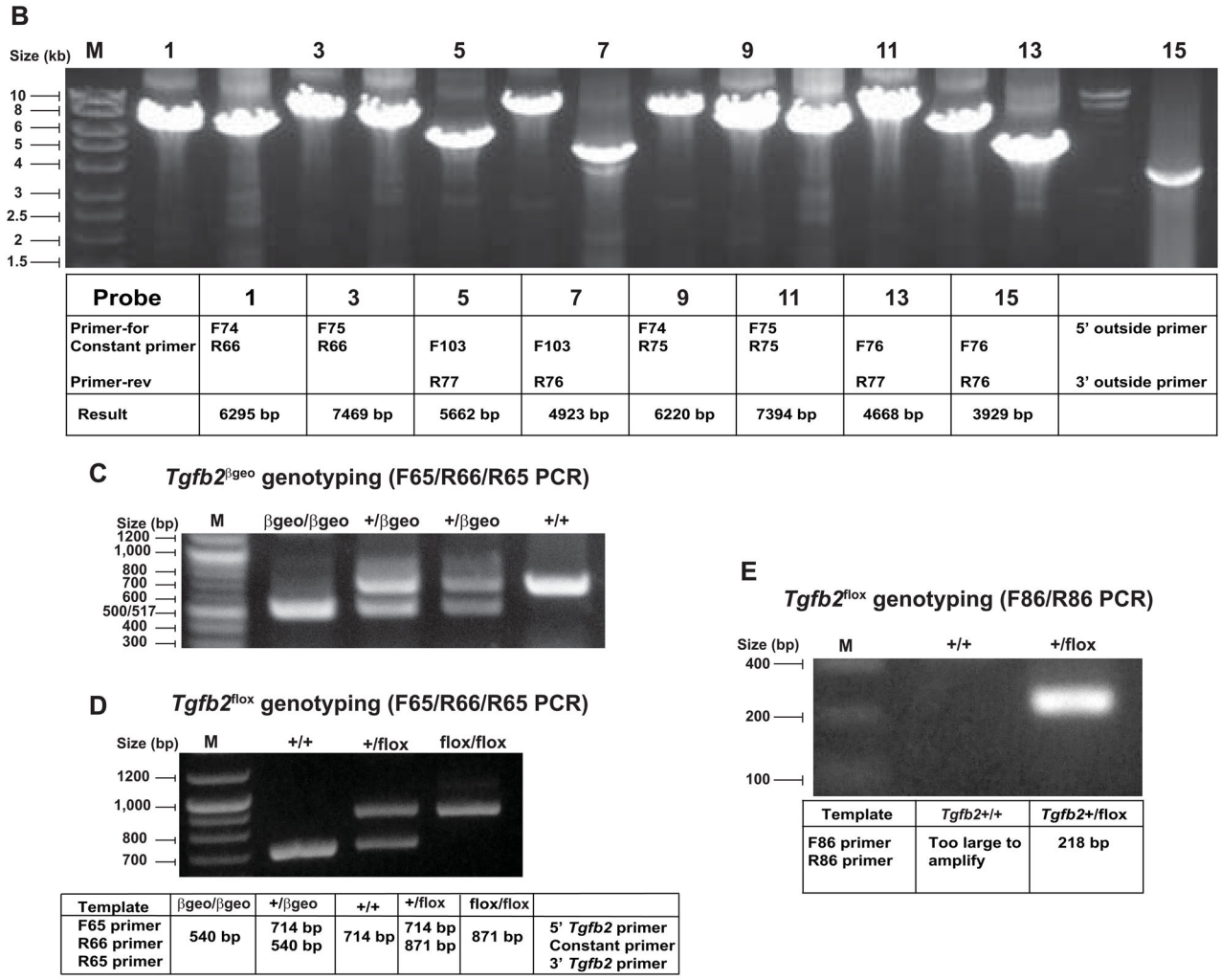

Probe	1	3	5	7	9	11	13	15	
Primer-for Constant primer	F74 R66	F75 R66		F103	F103	F74 R75	F75 R75	F76	F76	5' outside primer
Primer-rev				R77	R76			R77	R76	3' outside primer
Result	6295 bp	7469 bp		5662 bp	4923 bp	6220 bp	7394 bp	4668 bp	3929 bp	

Template	βgeo/βgeo	+/βgeo	+/+	+/flox	flox/flox	
F65 primer R66 primer R65 primer	540 bp	714 bp 540 bp	714 bp	714 bp 871 bp	871 bp	5' *Tgfb2* primer Constant primer 3' *Tgfb2* primer

Template	*Tgfb2*+/+	*Tgfb2*+/flox
F86 primer R86 primer	Too large to amplify	218 bp

Figure 1. Gene targeting scheme for generating mice with a knockout-first, *lacZ*-tagged insertion and conditional allele of *Tgfb2*

A: Schematic diagram of the *Tgfb2* wild-type, targeted knockout-first and *lacZ*-tagged insertion (*Tgfb2*$^{\beta geo}$), conditional (*Tgfb2*^{flox}), and conditional knockout (*Tgfb2*^{cko}) allele. Boxes with numbers represent exons. Both left and right homology arms in the targeting vector are clearly indicated. The 5′ outside and 3′ outside regions of the *Tgfb2* locus are shown in dotted lines. The targeting vector is designed to flank exon 2 with *loxP* to create *Tgfb2* conditional deletion through Cre-mediated recombination. The targeted *Tgfb2*$^{\beta geo}$ allele contains an IRES:*lacZ* trapping cassette and a floxed promoter-driven *neomycin* cassette inserted into the intron 1 of the *Tgfb2*. The presence of an Engrailed (En2) splice acceptor (SA) disrupts gene function, resulting in a *lacZ* fusion for studying gene expression localization. Splicing events are depicted in dotted lines. Flp recombinase can remove the *FRT* flanked gene trap cassette, convert the *Tgfb2*$^{\beta geo}$ allele to a conditional *Tgfb2*^{flox} allele and restore the TGFβ2 activity. Subsequent exposure to Cre recombinase can delete the floxed exon 2 of the *Tgfb2*^{flox} allele resulting in a *Tgfb2*^{cko} allele. All LR-PCR and genotyping screening primers are indicated by arrowheads. Drawn roughly to scale, the area,

to the left and right of different alleles, beyond the vertical curved lines is not drawn to the scale.

B: Long range PCR screening. LR-PCR screening of targeted ES cells is done using 8 different sets of 5′-outside or 3′-outside LR-PCR primers in combination with the constant cassette primers located within the targeting vector. Table indicates specific primer pairs and the observed large amplicon sizes, confirming the 5′ and 3′ end *Tgfb2*$^{\beta geo}$ targeting. M, DNA marker.

C: PCR genotyping of fetuses with wild-type, heterozygous, and homozygous *Tgfb2*$^{\beta geo}$ alleles. The primers used are: *Tgfb2* intron 2 *forward* primer (F65), constant/cassette *lacZ reverse* primer (R66) and *Tgfb2* exon 2 *reverse* primer (R65). The F65 and R66 primers produce a PCR product of 540 bp from the *Tgfb2*$^{\beta geo}$ allele, whereas F65 and R65 primers give rise to a PCR product of 714 bp from the wild-type allele. Band size as measured by DNA size markers (M) is indicated.

D: PCR genotyping of *Tgfb2*^{flox} mice. *Tgfb2*$^{\beta geo}$ allele gives rise to *Tgfb2*^{flox} allele (post Flp), which is specifically identified by 871 bp band in a three primer (F65, R66, R65) PCR reaction. Band size as measured by DNA size markers (M) is indicated.

E: PCR genotyping with a *Tgfb2 forward* primer (F86) and constant/cassette primer (R86) produces a unique PCR band of 218 bp from the *Tgfb2*^{flox} allele but not wild-type or *Tgfb2*$^{\beta geo}$ alleles.

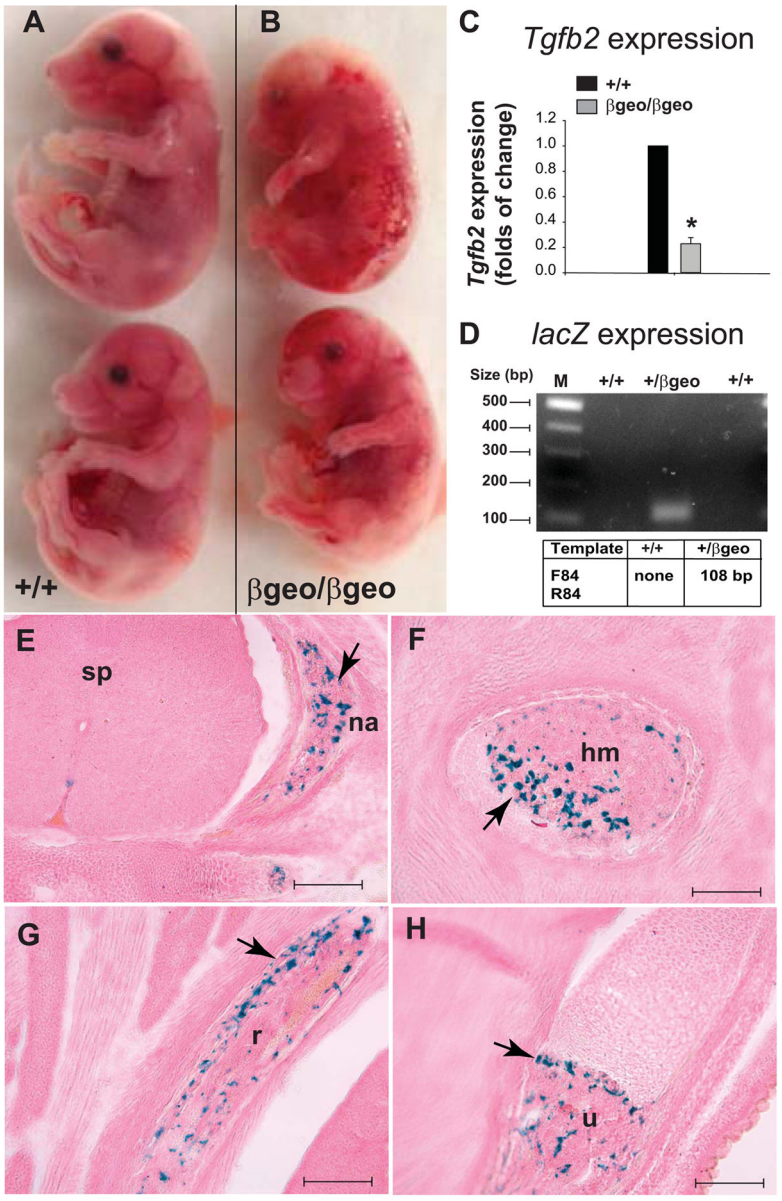

Figure 2. Gross morphological and molecular analyses of *Tgfb2*$^{\beta geo/\beta geo}$ fetuses

A–B: Gross morphological images of wild-type (A) and *Tgfb2*$^{\beta geo/\beta geo}$ (B) littermates at E17.5. *Tgfb2*$^{\beta geo/\beta geo}$ fetuses appear grossly abnormal with craniofacial features and excessive or abnormal blood vessels and profuse bleeding.

C: Real-time qPCR analysis of 'wild-type' *Tgfb2* expression in control and *Tgfb2*$^{\beta geo/\beta geo}$ fetal hearts. Total RNA from hearts of E16.5 fetuses is used to prepare the cDNA. Intron spanning Universal ProbeLibrary assay with a mouse *Tgfb2* exon 7 probe (#73) along with the *Tgfb2* exon 6 (forward) and *Tgfb2* exon 7 (reverse) primers are used for UPL qPCR analysis. Note that there is a significant loss of wild-type *Tgfb2* transcript expression in *Tgfb2*$^{\beta geo/\beta geo}$ fetal hearts (*P = <0.005, n = 3 for wild-type and *Tgfb2*$^{\beta geo/\beta geo}$). Expression levels are normalized to *β-actin* (via dual-color UPL real-time qPCR) and to the wild-type value.

D: Gel RT-PCR analysis indicates *lacZ* expression in *Tgfb2*$^{+/\beta geo}$ fetal hearts. Note that *lacZ* PCR fails as the *lacZ* cassette is absent in wild-type sample.

E–H: *lacZ* staining of X-gal for cryo-section of *Tgfb2*$^{+/\beta geo}$ fetues at (E16.5). The β-galactosidase staining indicated by blue color (arrow, E–H) is clearly visible in the ossified cartilage primordium of the neural arch (E), mid shaft region of left humerus (F), rib (G), and distal part of shaft of right ulna (H). Scale bar (E–H) = 200 μm. Abbreviations: na, neural arch; hm, humerus; r, rib; u, ulna.

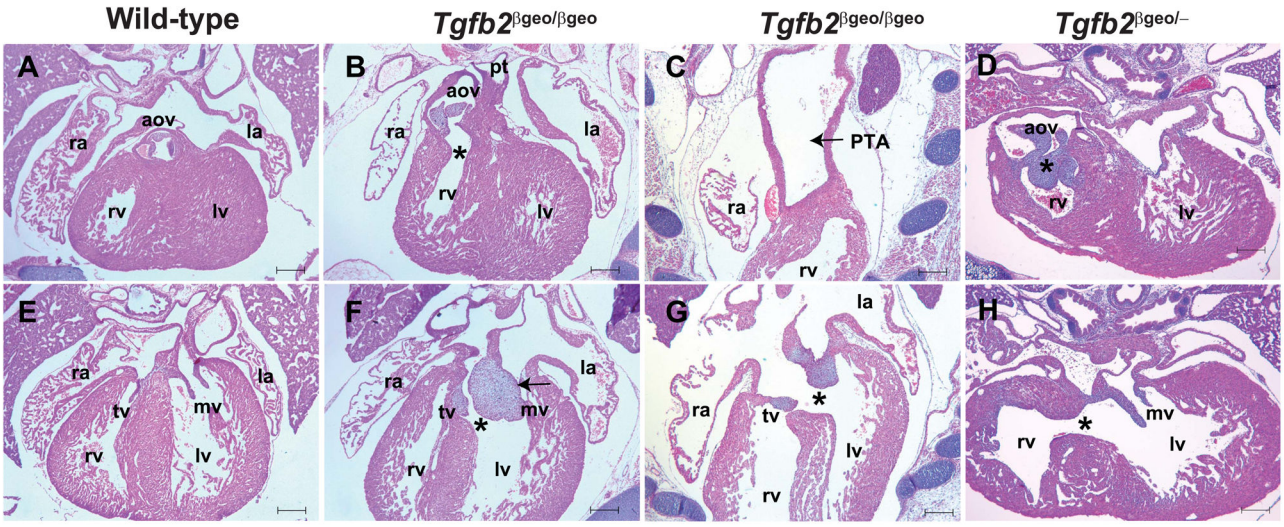

Figure 3. *Tgfb2*$^{\beta geo/\beta geo}$ and *Tgfb2*$^{\beta geo/-}$ fetuses develop similar cardiac structural defects

A–H: Hematoxylin and eosin (H&E) staining of wild-type (A, E), *Tgfb2*$^{\beta geo/\beta geo}$ (B–C, F–G), and *Tgfb2*$^{\beta geo/-}$ (D,H) fetuses at E17.5. *Tgfb2*$^{\beta geo/\beta geo}$ fetuses have double-outlet right ventricle (DORV) (asterisk, B) and thickened aortic valves (B), persistent truncus arteriosus (PTA) (arrow, C), double-inlet left ventricle (F, asterisk) and overriding tricuspid valve orifice via a perimembranous ventricular septal defect (VSD) (asterisk, G), and abnormally thickened mitral (arrow, F) and tricuspid valves (F,G). *Tgfb2*$^{\beta geo/-}$ fetuses show many similar cardiac malformations including DORV, VSD, and thickening of semilunar and mitral valves (D,H). Scale bars =200 μm for A–H. Abbreviations: rv, right ventricle; lv, left ventricle; pt, pulmonary trunk; aov, aortic valves; tv, tricuspid valves; mv, mitral valves; ra, right atrium; la, left atrium

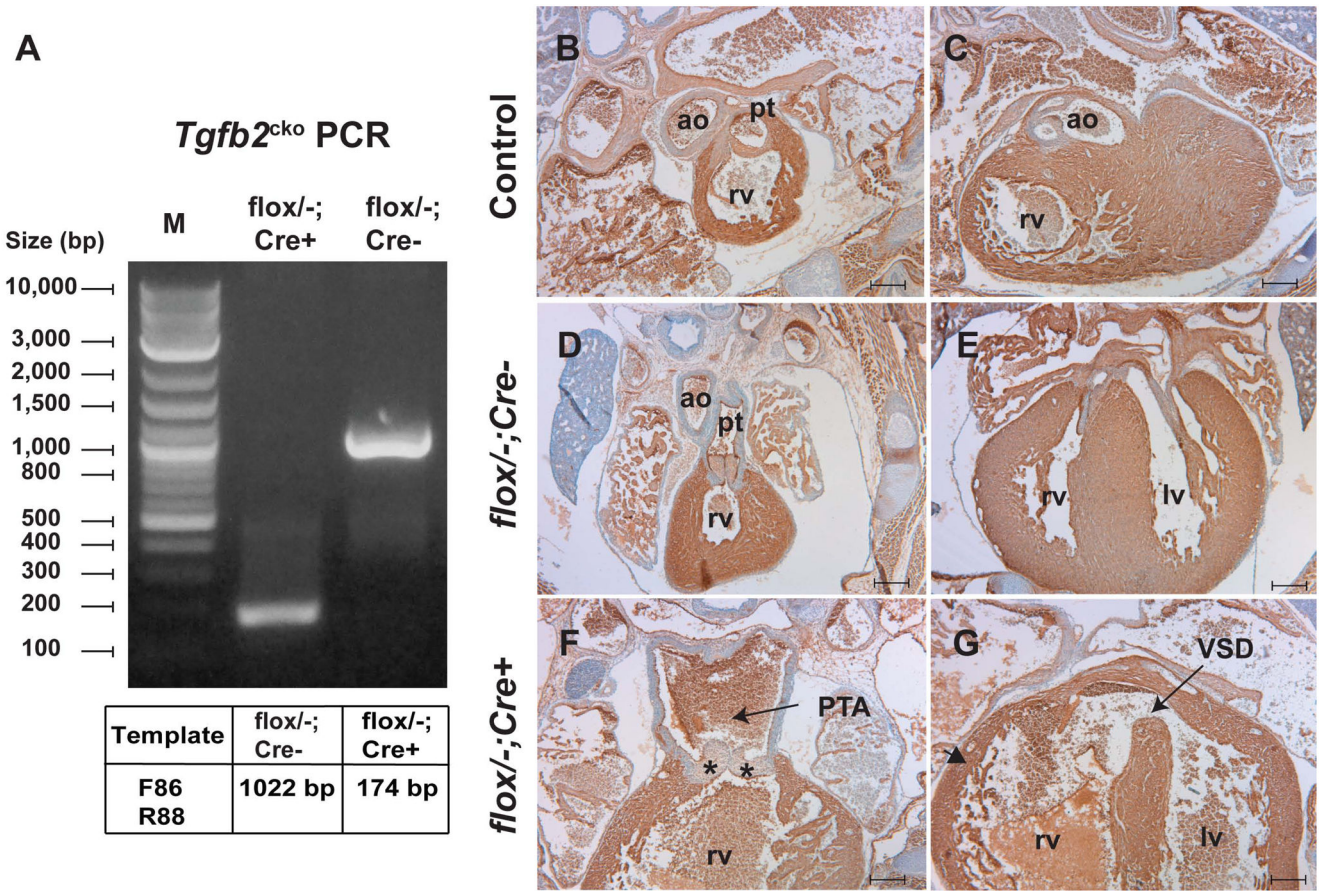

Figure 4. Systemic *Tgfb2* conditional knockout (*Tgfb2*^{cko}) fetuses develop congenital heart defects

A: Genomic PCR analysis of tail DNA samples indicating the Cre recombinase mediated *in vivo* deletion of *loxP* flanked exon 2 containing region of the *Tgfb2* in *Tgfb2*$^{flox/-}$;*EIIaCre*$^{+}$ but not *Tgfb2*$^{flox/-}$;*EIIaCre*$^{-}$ fetuses. Cre-mediated deletion of *Tgfb2*^{flox} allele results in a 174 bp band.

B–G: Cardiac morphology of wild-type (B–C), *Tgfb2*$^{flox/-}$;*EIIaCre*$^{-}$ (D–E), and *Tgfb2*$^{flox/-}$;*EIIaCre*$^{+}$ (F–G) is indicated by cardiac myosin heavy chain (MF20) immunohistochemistry at E17.5. Tissue sections are counterstained with hematoxylin. *Tgfb2*$^{flox/-}$;*EIIaCre*$^{-}$ (D–E) hearts are normal. Interestingly, *Tgfb2*$^{flox/-}$;*EIIaCre*$^{+}$ fetuses develop severe malformations of the cardiac outflow tract (F) (arrow, PTA; asterisks, abnormally thickened trucal valves) and inflow tract (G) (arrow, VSD; arrowhead, abnormal myocardium). These cardiac malformations are similar to the ones that are seen in the *Tgfb2*$^{\beta geo/\beta geo}$, *Tgfb2*$^{\beta geo/-}$, *Tgfb2*$^{-/-}$ fetuses. Scale bar =200 μm for B–G. Abbreviations: rv, right ventricle; lv, left ventricle; pt, pulmonary trunk; ao, aorta; PTA, persistent truncus arteriosus; VSD, ventricular septal defect